Seasonal and diurnal variation of marine wind characteristics based on lidar measurements

Shu, Z. R.; Li, Q. S.; Chan, P. W.; He, Y. C.

RESEARCH ARTICLE

Seasonal and diurnal variation of marine wind characteristics based on lidar measurements

Z. R. Shu[1] | Q. S. Li[2] | P. W. Chan[3] | Y. C. He[4]

[1]Department of Civil Engineering, University of Birmingham, Birmingham, UK

[2]Department of Architecture and Civil Engineering, City University of Hong Kong, Kowloon, Hong Kong (SAR), China

[3]Hong Kong Observatory, Kowloon, Hong Kong (SAR), China

[4]Joint Research Center for Engineering Structure Disaster Prevention and Control, Guangzhou University, Guangzhou, China

Correspondence
Yuncheng He, Joint Research Center for Engineering Structure Disaster Prevention and Control, Guangzhou University, Guangzhou, China.
Email: yuncheng@gzhu.edu.cn

Funding information
Education Bureau of Guangzhou, China, Grant/Award Number: 201831834

Abstract

The accurate assessment of marine wind characteristics is receiving increasing attention because of its practical importance in diverse areas. However, the reliable measurement of marine winds is often insufficient mainly because of the limitation of the instrumentation used. In the present study, four year lidar measurement data, recorded continuously from March 2012 to November 2015, are collected at an offshore platform near Lamma Island in Hong Kong, China, to obtain useful marine meteorological information, with a particular interest in the seasonal and diurnal variations of wind speed, wind shear co-efficient (WSC) and veering wind angle. It is shown that the wind speed and Weibull parameters generally exhibit evident monthly variation. The maximum monthly wind speed occurs in February, with values between 7.41 and 8.13 m·s^{-1} depending on the height, and the monthly minimum occurs in August, with values between 4.66 and 5.27 m·s^{-1}. The Weibull scale parameter shows a similar monthly pattern with wind speed, while the Weibull shape parameter peaks in June. Furthermore, the diurnal pattern of both wind speed and Weibull parameters is closely tied to seasonality. The WSC covering the bottom and top layers of the wind turbine is likewise examined. Larger WSCs are obtained during hotter months, while smaller WSCs are associated with cooler months. The diurnal pattern of the WSC shows reasonable agreement among different seasons, although the magnitude is somewhat different. The veering angle generally increases with height. Its monthly pattern reveals a maximum in May, reaching up to 17.8° within the height of concern. Pronounced monthly and diurnal patterns of veering angles are observed at higher altitudes.

KEYWORDS
marine wind characteristics, seasonal and diurnal variation, veering angle, wind lidar, wind shear co-efficient, wind speed

1 | INTRODUCTION

The characteristics of wind within the atmospheric boundary layer (ABL) are of paramount interests for many engineers and researchers since they form a decisive factor relating to the engineering practices of diverse areas, such as the investigation of the wind effects on structures (i.e., buildings, bridges and

transmission towers), the assessment of the safety and comfort of pedestrians and cyclists near buildings, the prediction of wind power and the economic feasibility of wind turbines, an investigation into the lodging resistance of various crops, as well as the evaluation of the dispersion of air contaminants. There is clear evidence in numerous observational and modelling studies that many atmospheric quantities, such as wind, precipitation, surface pressure, cloudiness and radiation fluxes, are subject to a distinct diurnal variation process, which is driven mainly by the daily cycle of solar radiation at the top of the atmosphere (Yu *et al.*, 2009). Under such circumstances, understanding the diurnal cycle of wind is essential with regard to the aforementioned practices.

The diurnal pattern of wind speed has been well documented in the existing literature. It generally displays a maximum during the early afternoon and a minimum during night-time (Crawford and Hudson, 1973; Dai and Deser, 1999; Arya, 2001; Yu *et al.*, 2009; Fajber *et al.*, 2014). Such a daily pattern is a surface-driven phenomena attributed mainly to the oscillation of the transfer of momentum. The daily maximum occurring at midday is mostly because of the increased downward transfer of momentum as a result of increased thermal mixing, while during the night-time, when radiative cooling dominates, a stable boundary layer is formed that prevents the transfer of momentum, thus leading to relatively calm winds at the near-surface level (Arya, 2001). In addition, He *et al.* (2012, 2013) showed that not only the mean but also the probability distribution and fractal dimension of near-surface wind speeds reveal a clear diurnal cycle. Shu *et al.* (2015a) reported that the diurnal pattern of wind speed is closely tied to terrain conditions. The daily maximum for city-centre stations occurs during the early afternoon, while a daily minimum is found at hill-top stations during the same period. Kodama *et al.* (1989) noted that the daily maximum at a low level is strongly dependent on the change in baroclinicity.

It is worth noting that the literature summarized above mainly focuses on the wind characteristics for overland conditions, while the understanding of marine winds is comparatively limited. The wind characteristics at offshore sites are more complicated compared with those for overland conditions. Offshore wind generally has a higher wind speed, with less turbulence and wind shear. Besides, the vertical thermal mixing that dominates the daily pattern of wind speed for overland conditions is less significant at offshore sites because of the large thermal capacity of the water. Thus, the sea-surface temperature is more likely to remain stable (Barthelmie *et al.*, 1996).

In this case, the near-surface wind variation under marine conditions is associated predominantly with the horizontal land–sea thermal contrast. On the other hand, the stable sea-surface temperature is conducive for the generation of convective heat fluxes in overlying flows because of advective changes. Hence, the diurnal oscillation of marine wind speed is jointly affected by the diurnal changes of land–sea thermal contrast and the advective changes over the sea (Lapworth, 2005, 2011). Furthermore, the frequent occurrence of some diurnally varying flows in the marine area, such as sea breezes and the coastal jet, could potentially cause the diurnal oscillation of marine winds (Lapworth, 2005).

Given the complexity involved in the mechanism governing the marine ABL, the diurnal cycle or, more broadly, the behaviour of the marine wind, is expected to be somewhat different with overland winds. Barthelmie *et al.* (1996) and Yu and Wagner (1970) found that in many marine wind observational studies, the diurnal oscillation of surface wind speed is more or less consistent with those observed under overland conditions. However, there is also a considerable amount of evidence showing that an inverted diurnal cycle for wind speed may occur for marine winds, where surface wind speed reaches a maximum overnight and a minimum during the daytime (Yu and Wagner, 1970; Barthelmie, 1991; Barthelmie *et al.*, 1996; Lapworth, 2005, 2011). Such a deviation is potentially related to the difference of fetch distance (Yu and Wagner, 1970; Barthelmie *et al.*, 1996).

It is important to note that the accurate assessment and quantification of marine meteorological information is of essential importance related to a wide range of offshore engineering practices, such as the daily weather forecast and navigation safety surveys, but also in atmospheric and oceanographic studies, as well as in offshore energy harvesting (Launiainen and Laurila, 1984). However, physically and statistically representative data for marine winds are often insufficient because of various practical difficulties. Given the limited literature with relevance to the seasonal and diurnal cycle of marine wind characteristics, the main objective of the study is to shed a light on the seasonal and diurnal characteristics of wind speed, wind shear co-efficient (WSC) and veering angle based on continuous four year lidar measurement data recorded at an offshore observational platform in Hong Kong.

The paper is structured as follows. Section 2 briefly overviews the measurement system, mainly including a site description and instrumentation. Section 3 presents the results and relevant discussions. Section 4 summaries the major outcomes and concludes.
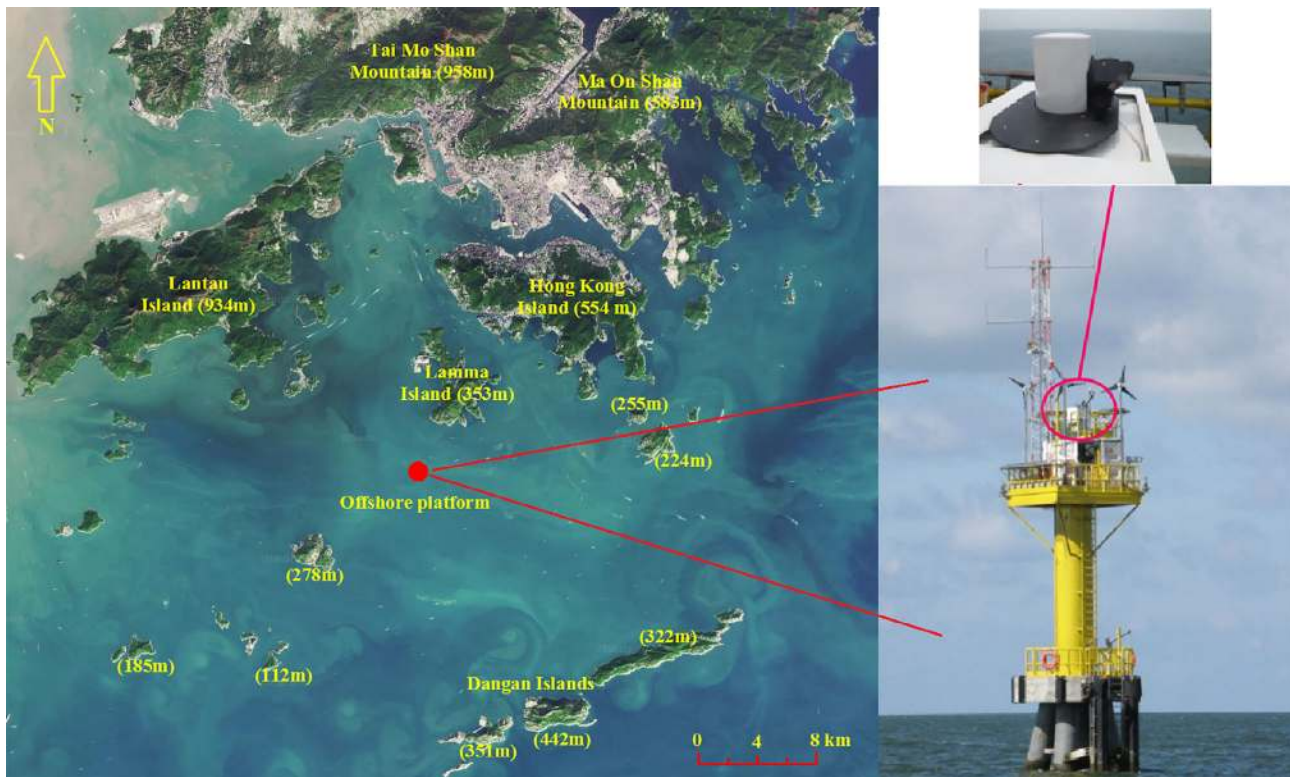
FIGURE 1 Site location of the offshore platform (highlighted by the solid circle) and measurement equipment

2 | SITE DESCRIPTION AND OBSERVATION INSTRUMENTATION

The data analysed were recorded by a light detection and ranging (lidar) system at an offshore observational platform near Lamma Island in Hong Kong, China (Figure 1). The platform is exposed to a fairly homogeneous open-water terrain within the range of 60–240° (He et al., 2019), while a few notable landmasses exist to its north, mainly including Lamma Island (3.5 km to its northeast), Cheung Chau Island (9 km to its northwest) and Lantau Island (15 km to its northwest).

It is noted that the wind lidar system has been extensively deployed for the quantification of marine wind characteristics because of its ability to provide high-quality, reliable wind measurement at different altitudes (Hasager et al., 2008; Pichugina et al., 2012; Shu et al., 2016). In the present study, the wind lidar measurement system was fixed at the southwest corner of the platform, with a base height of 20 m above mean sea level (AMSL). It is of a Galion Lidar Unit type (distributed by SgurrEnergy) with a measurement capacity $> 40 \text{ m} \cdot \text{s}^{-1}$ at a resolution $< 0.1 \text{ m} \cdot \text{s}^{-1}$. The Galion Lidar is a pulsed laser device with the capability to provide simultaneous measurements of wind speed and direction at several levels. Typically, the wind lidar system omits laser pulses that are reflected by

aerosols in the atmosphere, and the along-beam velocity can be determined from the frequency shift using the Doppler equation (Hofsäß et al., 2018). During the measurement campaign, the wind lidar was configured to operate in velocity azimuth display (VAD) mode, in which the azimuth angle is varied over a circle with a fixed elevation angle. In order to compare and validate the lidar measurements with nearby mast measurements, data filtering was applied to the original high-resolution lidar data by means of wind field reconstruction and a carrier-to-noise (CNR) filter. The accuracy of lidar measurements was well validated by comparison with their mast counterpart located nearby, and it exhibited satisfactory agreement.

The lidar measurement campaign was carried out continuously between March 2012 and November 2015. Statistical estimates of the mean, standard deviation (SD), and minimums and maximums for horizontal wind speed, as well as the mean and SD of wind direction were updated every 10 min at 17 gates, ranging from 21.3 to 178.3 m AMSL.

3 | RESULTS AND DISCUSSIONS

3.1 | Data processing and quality control

To take into account the fact that the fidelity of 10 min lidar profiler measurement is sometimes subject to

certain uncertainties because of environmental and inherent factors, a data quality-control procedure is performed in the initial stage to remove erroneous and invalid measurements (He *et al.*, 2019). In the current study, a threshold of 12 scans was required to produce valid statistics of wind measurement at a specific altitude within each individual 10 min profile measurement.

In order to enhance the reliability of the result, the analysis was mainly carried out from a statistical point of view using a composite analysis in which all qualified data corresponding to the specific category were assembled and averaged. Moreover, Hong Kong is located in a typhoon-prone region frequently under the influence of non-synoptic events, such as tropical cyclones. Under such circumstances, the lidar measurement data recorded during the passage of these strong wind events were specifically removed in the following analysis.

3.2 | Wind speed

For the assessment of marine wind characteristics, the diurnal cycle of mean wind speed is often of primary interest because it is a decisive factor in numerous engineering applications. According to the existing literature, overland winds typically exhibit a maximum slightly after midday and a minimum during night-time, whereas an inverted diurnal variation pattern may occur for marine winds. In the current study, the monthly variation of mean wind speed at selective altitudes was first performed as illustrated in Figure 2. It is apparent that the mean wind speed is strongly dependent on the change of seasonality. The monthly mean wind speed generally exhibits a maximum in February, followed by a monotonic decrease and reaches a minimum in August. A second maximum is also found around November. The enhanced wind speed between November and February is associated primarily with the occurrence of a strong northeast monsoon during the winter in Hong Kong.

Since the wind speed measurement recorded at the offshore site is subject to evident seasonality, it is therefore reasonable to investigate the diurnal cycle of mean wind speed as a function of different seasons (Figure 3). For transparency, the four seasons are defined by following previous studies (Shu *et al.*, 2015a, 2015b) as: spring (March–May), summer (June–August), autumn (September–November) and winter (December–February). As would be expected, the diurnal pattern of wind speed changes in response to the change in seasonality. It is clearly shown that the diurnal variation of wind speed is more pronounced during summer and autumn, while the wind speeds during winter and spring remain somewhat constant. For summer, the wind speeds are
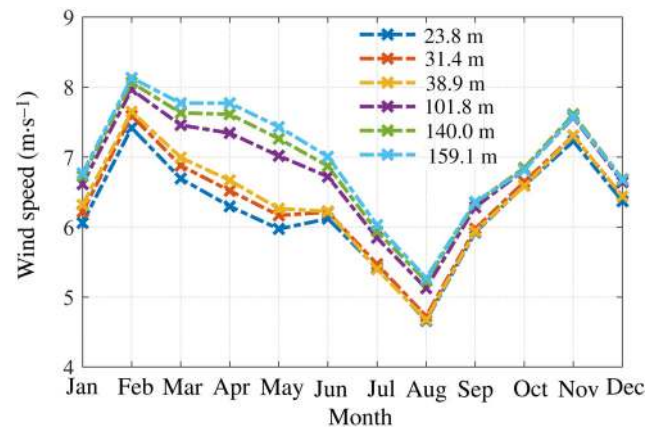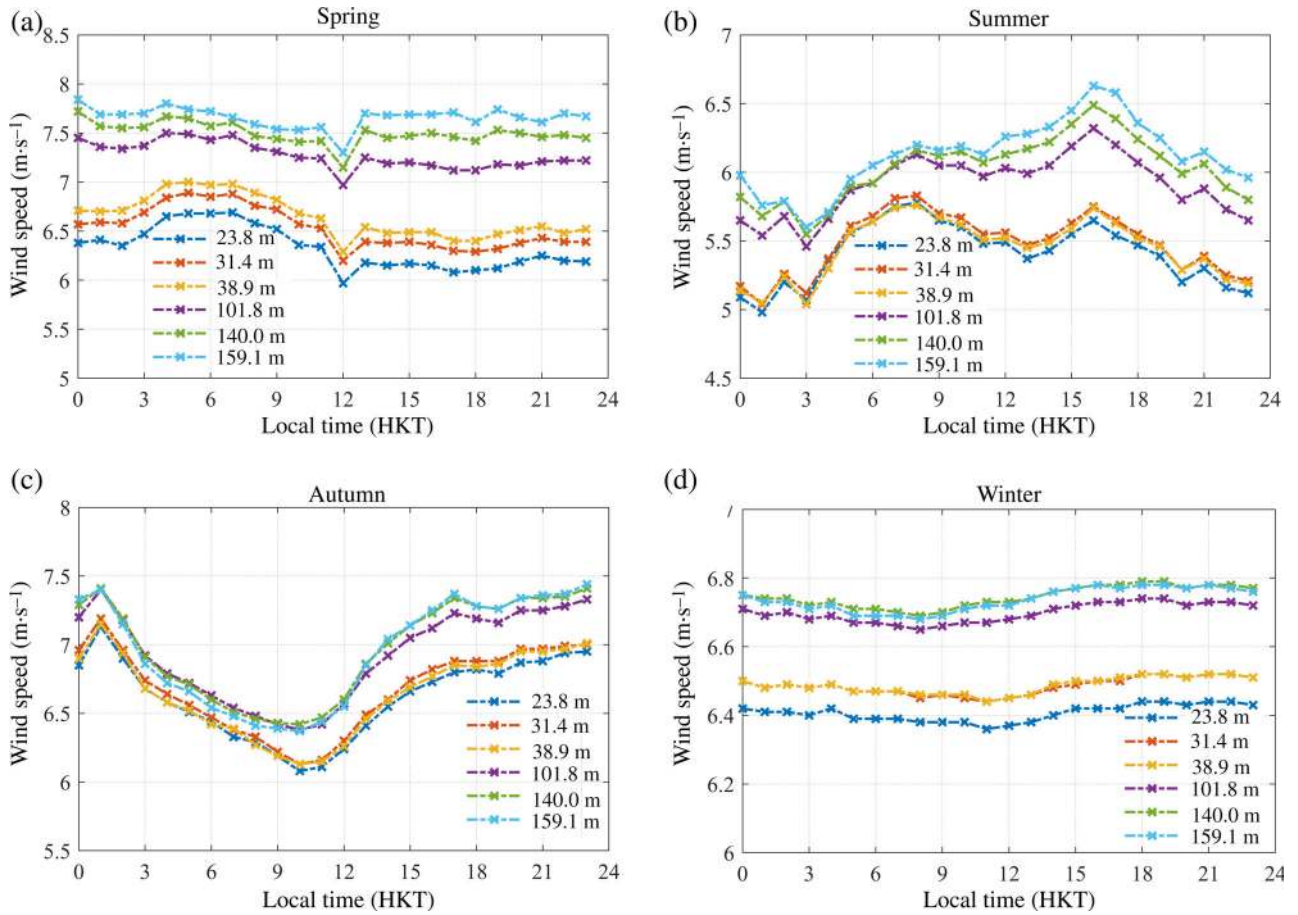

FIGURE 2 Monthly variation of the mean wind speed at different altitudes

generally higher during the daytime (0800–1600 hours), featuring two maxima at, respectively, 0800 and 1600 hours. There appears to be a slight decrease in wind speed around 1200–1300 hours. On the contrary, the wind speeds during autumn also indicate a salient diurnal cycle, which, however, differs remarkably with that of summer winds. The autumn wind speeds are much lower during the daytime, reaching a minimum slightly before 1200 hours and an increase afterwards. It is noteworthy that the summer daily pattern is somewhat similar to those observed for overland condition, while the wind speed in autumn displays a nearly reverse daily pattern. This is attributed mostly to the difference in the land–sea thermal contrast.

In order to facilitate further offshore wind harvesting, a statistical analysis of marine wind speeds at different altitudes was performed using a two-parameter Weibull distribution function. The Weibull distribution function has been applied almost unanimously in the wind energy industry in order to characterize the statistical properties of wind speed and to evaluate potential wind energy (Shu *et al.*, 2015a; 2015b; 2016):

$$f(V) = \left(\frac{k}{c}\right)\left(\frac{V}{c}\right)^{k-1} \exp\left[-\left(\frac{V}{c}\right)^k\right] \quad (v>0; k,c>0) \quad (1)$$

where $f(V)$ is the probability of observed wind speed V; c is the Weibull scale parameter (m·s^{-1}); and k is the dimensionless Weibull shape parameter. Essentially, the scale parameter c is an indicator of how windy the location is, while the shape parameter k describes the width of the data distribution which indicates how peaked the distribution is. The Weibull parameters are determined based on the mean (V_m) and standard deviation (σ) of wind speeds using the following relations:

**FIGURE 3** Diurnal variation of the mean wind speed at different altitudes
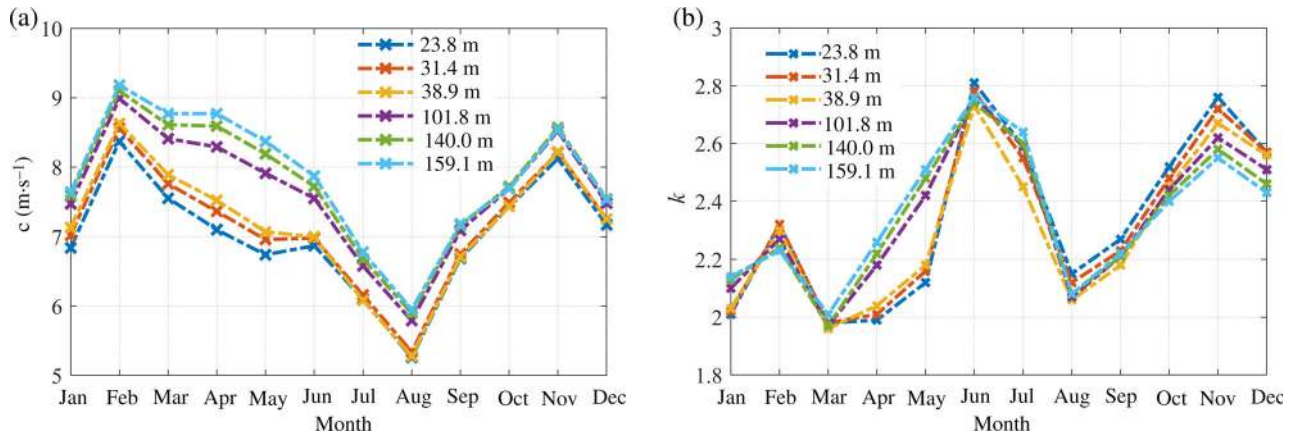
FIGURE 4 Monthly variation of the Weibull scale (c) and shape (k) parameters at different altitudes

$$k = \left(\frac{\sigma}{V_m}\right)^{-1.086} \quad (1 \le k \le 10) \tag{2}$$

$$c = \frac{V_m}{\Gamma(1 + 1/k)} \tag{3}$$

Likewise the mean wind speed, the variation in the Weibull parameters is also examined on monthly and diurnal bases (Figure 4–6). The monthly variation in the Weibull scale parameter (Figure 4) is more or less similar to that of mean wind speed (Figure 2), with two maxima occurring in February and November, respectively, and a minimum in August. The monthly variation of the Weibull shape parameter, on the other hand, appears to be much more complicated: two maxima are found in June and November.
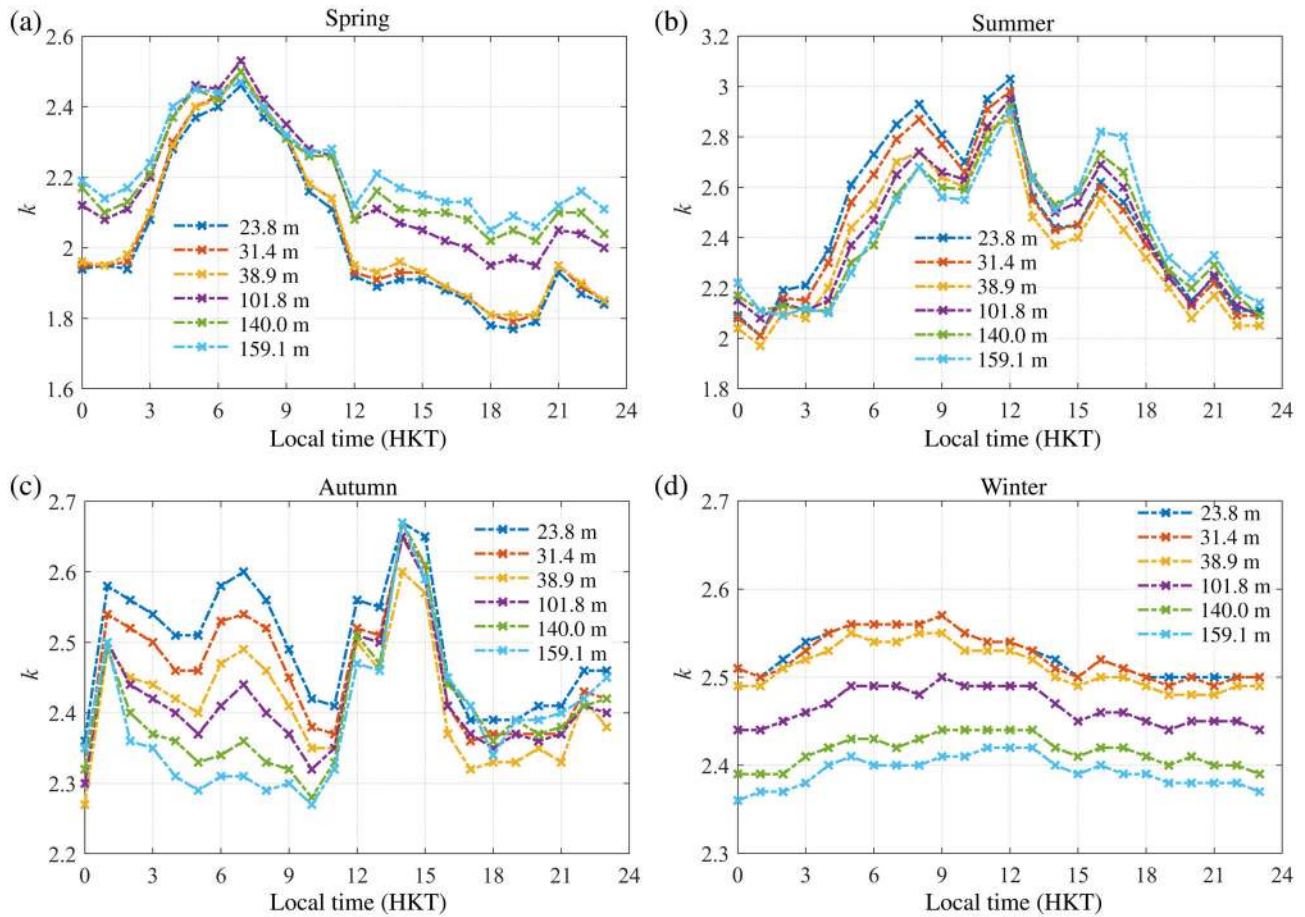
FIGURE 5 Diurnal variation of the Weibull shape parameter at different altitudes

For the Weibull shape parameter, the diurnal variation pattern (Figure 5) has a strong dependence on seasonality. During spring, it has a salient maximum at around 0700 hours, followed by a continuous decrease. Meanwhile, it is noteworthy that the magnitude of the shape parameter appears to be independent of height between 0300 and 0900 hours, while outside this period, the shape parameters at higher altitudes are larger than those at lower levels. For summer winds, the Weibull shape parameter is generally higher during daytime, and the magnitude remains somewhat constant regardless of the change of measurement altitude. For autumn winds, it is interesting that the shape parameter between 0200 and 1100 hours is apparently height dependent, the magnitude of which tends to decrease with increasing altitude, while during the remaining hours the shape parameter is more likely to be invariant with altitude. The diurnal variation of the Weibull shape parameter during winter is relatively moderate as compared with those in other seasons. The diurnal variation of the Weibull scale parameter (Figure 6) associated with different seasons is consistent with that of mean wind speed. The diurnal cycles during spring and winter are much

less pronounced, while summer and autumn winds show two evidently different types of diurnal pattern.

3.3 | Wind shear co-efficient (WSC)

In addition to wind speeds, the study is also concerned with the seasonal and diurnal characteristics of the WSC. It is a useful parameter in various branches of wind engineering, among which the use of the WSC for the extrapolation of wind speed from the available measurement altitude to the hub height of the wind turbine is arguably one of the most well-known applications. The WSC is essentially a handy parameter used to describe the dependence of horizontal wind speed on height, which is typically calculated as:

$$\alpha = (\ln v_2 - \ln v_1)/(\ln z_2 - \ln z_1) \qquad (4)$$

where v_2 and v_1 are the horizontal wind speeds at altitudes z_2 and z_1. In the wind energy community, the one-seventh power law model has been extensively applied to estimate the wind speed at hub height, which, however, is sometimes questioned since the magnitude of the WSC is usually
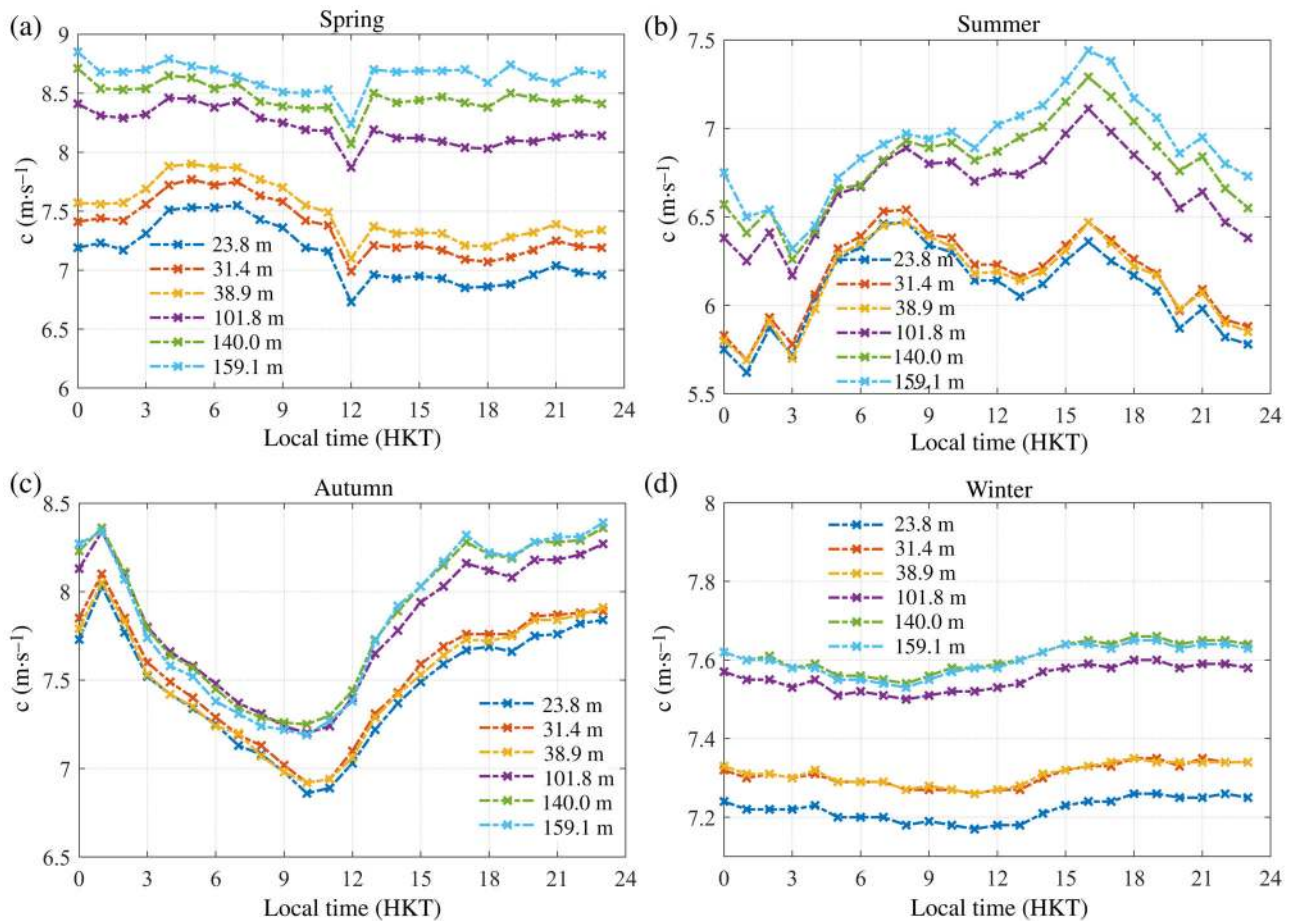
FIGURE 6 Diurnal variation of the Weibull scale parameter at different altitudes

TABLE 1 Wind shear co-efficients (WSCs) calculated in the current study

Wind shear between ...	Symbol
80.23 and 41.52 m	α_1
120.67 and 80.23 m	α_2
159.10 and 120.67 m	α_3

non-constant and may vary depending on many factors, such as thermal stability, terrain conditions and wind speed.

In the current study, three different types of WSCs were calculated (Table 1) that fully cover the bottom and top layers of the hub height of most existing wind turbines (i.e., 100 m). Figure 7 reveals the variation of the WSC on a monthly basis. Although these WSCs may differ sometimes in magnitude, the overall monthly variation patterns are in good agreement, featuring a maximum around April/May and a minimum during the cooler months of October–February. The magnitude of the WSC, particularly during hotter months (May–August), decreases as altitude increases.

Likewise, Figure 8 depicts the diurnal cycle of the WSC as a function of seasonality. For spring winds, the

WSCs generally reach a minimum during early morning (0500–0800 hours), while they remain relatively constant after 1300 hours. The WSC stays positive over the entire diurnal cycle, suggesting that wind speed always increases with altitude. While the WSC at lower altitudes continues to remain positive (i.e., α_1, α_2) during summer, a negative WSC starts to occur at higher altitudes (i.e., α_3), mostly between 0300 and 1200 hours. This is also the period in which the WSCs (i.e., α_1, α_2, α_3) deviate the most. The occurrence of a negative WSC indicates a decrease in wind speed with increasing altitude, suggesting the appearance of a jet-like wind speed maximum at the corresponding altitude. During autumn, the period in which a negative WSC occurs extends further, spanning from 0000 to 1300 hours. Meanwhile, the maximum negative WSC also increases from −0.065 in summer to −0.102 in autumn. For winter winds, the diurnal variation of the WSC, regardless of the altitude (i.e., α_1, α_2, α_3), is somewhat small as compared with those in other seasons. The α_3 tends to be negative over the entire diurnal cycle with an average of about −0.009, which can be partly attributed to the low-level jets resulting from the frequent passage of the strong northeast winter monsoon (Shu et al., 2018a).
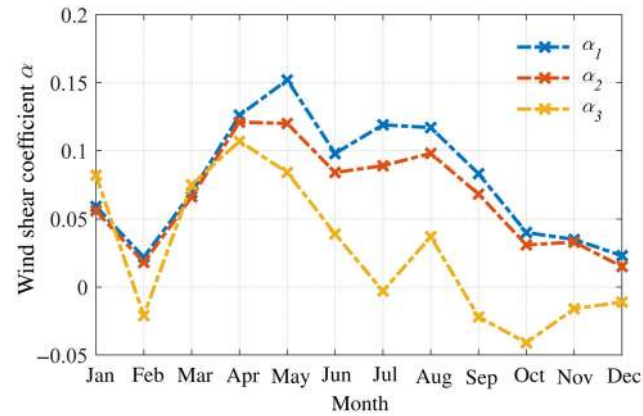
3.4 | Veering wind angle

The seasonal and diurnal variations of marine wind characteristics were investigated in terms of veering wind angle. A rich literature shows that the winds within the ABL always veer as a function of altitude mainly because of the Ekman layer effect (Yeo and Simiu, 2010; He *et al.*,

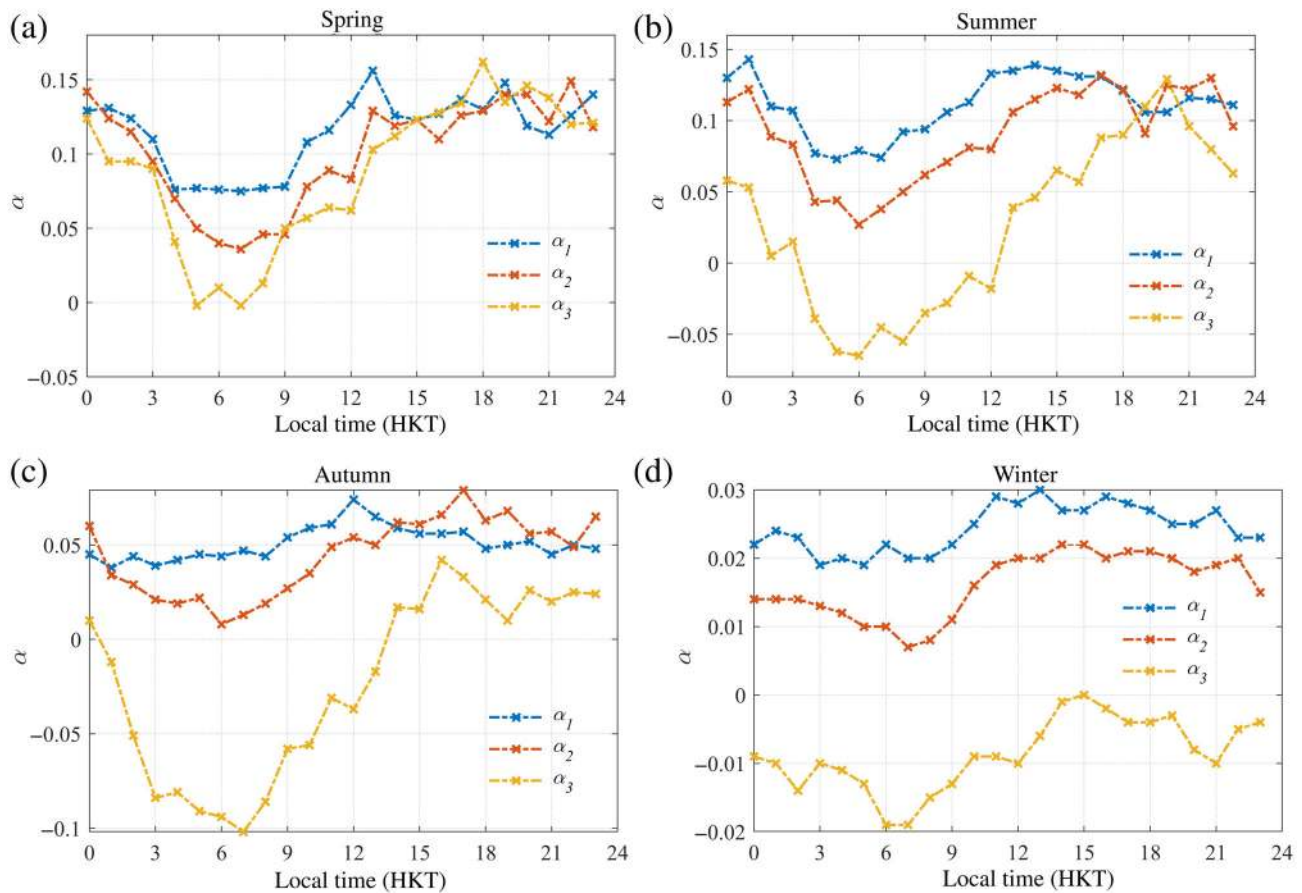**FIGURE 7** Monthly variation of the wind shear co-efficient (WSC) at different altitudes

2016; Shu *et al.*, 2018b), although such a phenomenon has received very little attention in wind engineering practices. Nonetheless, given the fast development of high-rise man-made structures, the veering of winds is receiving growing concern among structural designers and engineers. Particularly for wind energy development, as wind turbines become larger in size, it is reasonable to take into account the veering wind effect of the marine environment when concerned with both the design of fatigue loads and the economic feasibility of future wind turbines. In the present study, the veering of wind is quantified by the veering wind angle (i.e., $\Delta\theta$), which is simply defined as the difference in wind direction measurement between the altitude of interest (i.e., θ_i) and the lowest altitude of concern (i.e., $\theta_{23.8}$):

$$\Delta\theta = \theta_i - \theta_{23.8}\ (i = 31.4, 38.9, 101.8, 140.0, 159.1\,\text{m}) \quad (5)$$

Figure 9 illustrates the monthly variation of veering wind angle at different altitudes. It is apparent that the veering wind angle generally increases with altitude. The angles at lower altitudes show relatively weak monthly variation, while those at higher altitudes reveal a significant monthly maximum in May. Despite the deviation in
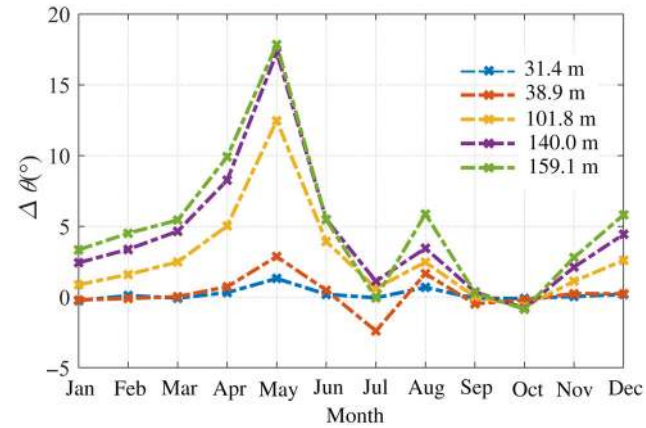

FIGURE 8 Diurnal variation of the wind shear co-efficient (WSC) at different altitudes

magnitude, the variation pattern among different altitudes is generally consistent. Furthermore, it is clear from Figure 10 that the diurnal variation of the veering wind angle is a function of seasonality. The diurnal cycle of the veering wind angle during spring and summer is somewhat similar, when the veering wind angles at lower altitudes vary

moderately, while those at higher altitudes typically have an early morning minimum at about 0300–0600 hours and a daily maximum after midday (i.e., 1500 hours). There appears to be a slight difference in the daily cycle after sunset (i.e., 1800 hours), where the veering wind angle during spring tends to decrease but increase during summer. Moreover, the veering wind angle during spring and summer remains mostly positive, suggesting a clockwise rotation of the wind direction as a function of altitude. However, the anticlockwise rotation of the wind direction starts to show at higher altitudes during autumn, occurring mainly during the period between 0300 and 1200 hours, and the magnitude of the veering wind angle during night-time is higher than that during daytime. For winter winds, on the other hand, the veering wind angle tends to level off throughout the entire daily cycle.

FIGURE 9 Monthly variation of the veering angle at different altitudes

4 | CONCLUSIONS

The accurate understanding of marine wind characteristics is imperative and can be applied to many branches of
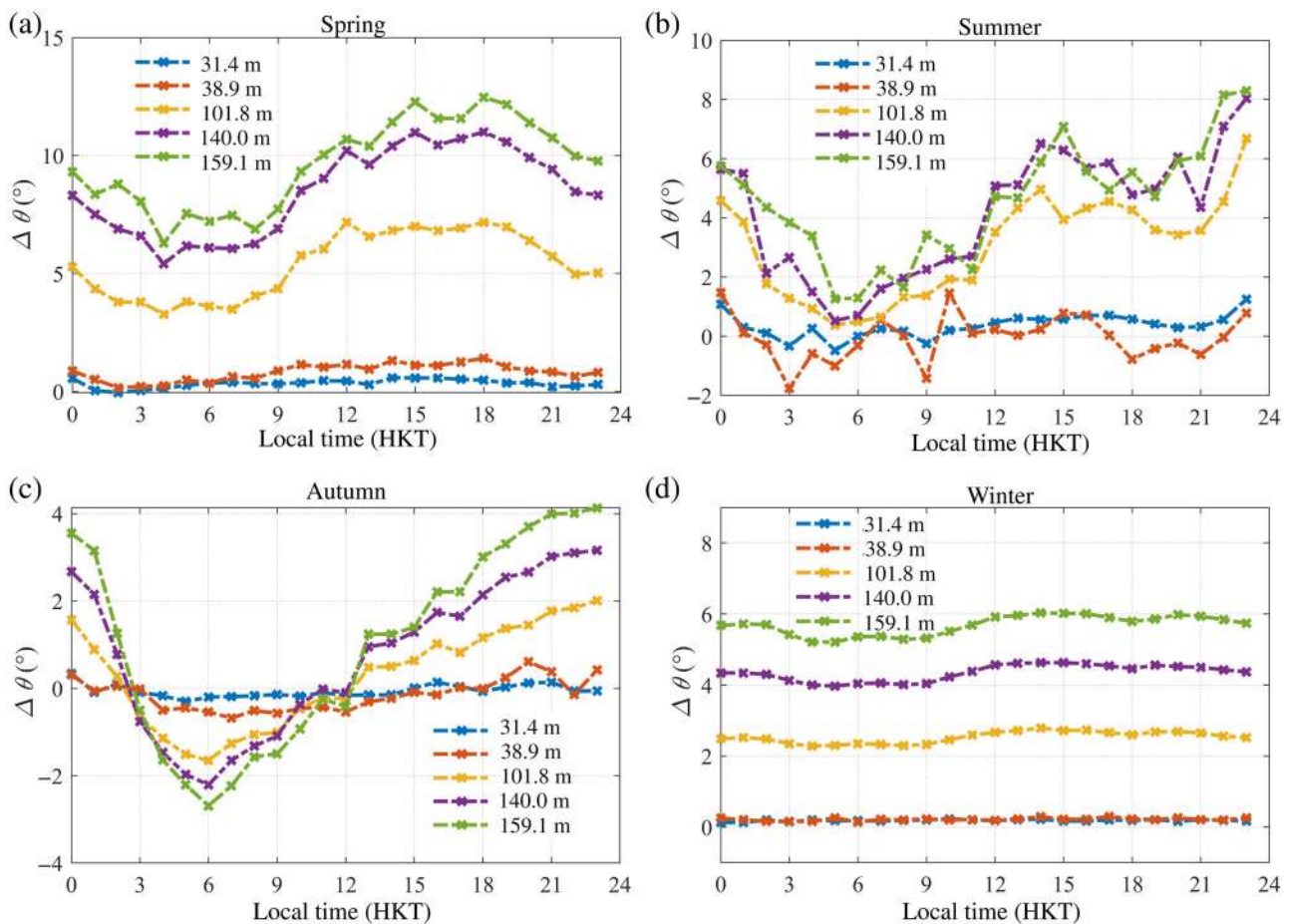
FIGURE 10 Diurnal variation of the veering angle at different altitudes

wind engineering practices. Accordingly, the study presents a comprehensive assessment of marine winds based on four year lidar measurement data recorded at an offshore platform in Hong Kong, China, with a particular interest in the seasonal and diurnal cycle of the mean wind speed, wind shear co-efficient (WSC) and veering wind angle. The major conclusions derived include the following:

- The mean wind speed generally shows monthly maxima in February and November, with a monthly minimum in August. The diurnal variation of the mean wind speed, on the other hand, shows no consistent pattern, which changes as a function of seasonality. Likewise, the Weibull parameters derived based on the mean wind speed also indicate a significant monthly variation, and their diurnal variability is markedly different among seasons.
- The WSC is generally highest during the hotter months and lowest during the cooler months. The diurnal pattern of the WSC, although it may differ in magnitude, shows reasonable agreement for shape among the seasons.
- The magnitude of the veering wind angle generally increases with altitude. While the veering wind angles at lower altitudes show only marginal monthly and diurnal variation, those at higher altitudes indicate evident variation with both monthly and diurnal bases. Furthermore, the diurnal cycle of the veering wind angle is also dependent upon seasonality.

ORCID
P. W. Chan https://orcid.org/0000-0003-2289-0609
Y. C. He https://orcid.org/0000-0002-6639-5901

REFERENCES
Arya, P.S. (2001) *Introduction to Micrometeorology*, Vol. 79. London, England: Academic press,

Barthelmie, R. (1991) *Predicting on- and off-shore wind speeds for wind energy applications*. Doctoral dissertation, University of East Anglia.

Barthelmie, R.J., Grisogono, B. and Pryor, S.C. (1996) Observations and simulations of diurnal cycles of near-surface wind speeds over land and sea. *Journal of Geophysical Research: Atmospheres*, 101(D16), 21327–21337.

Crawford, K.C. and Hudson, H.R. (1973) The diurnal wind variation in the lowest 1500 ft in Central Oklahoma. June 1966–May 1967. *Journal of Applied Meteorology*, 12(1), 127–132.

Dai, A. and Deser, C. (1999) Diurnal and semidiurnal variations in global surface wind and divergence fields. *Journal of Geophysical Research: Atmospheres*, 104(D24), 31109–31125.

Fajber, R., Monahan, A.H. and Merryfield, W.J. (2014) At what time of day do daily extreme near-surface wind speeds occur? *Journal of Climate*, 27(11), 4226–4244.

Hasager, C.B., Peña, A., Christiansen, M.B., Astrup, P., Nielsen, M., Monaldo, F. and Nielsen, P. (2008) Remote sensing observation used in offshore wind energy. *IEEE Journal of Selected Topics in Applied Earth Observations and Remote Sensing*, 1(1), 67–79.

He, Y., McFarlane, N.A. and Monahan, A.H. (2012) The influence of boundary layer processes on the diurnal variation of the climatological near-surface wind speed probability distribution over land. *Journal of Climate*, 25(18), 6441–6458.

He, Y.C., Chan, P.W. and Li, Q.S. (2013) Wind characteristics over different terrains. *Journal of Wind Engineering and Industrial Aerodynamics*, 131, 51–69.

He, Y.C., Chan, P.W. and Li, Q.S. (2016) Observations of vertical wind profiles of tropical cyclones at coastal areas. *Journal of Wind Engineering and Industrial Aerodynamics*, 152, 1–14.

He, Y.C., Fu, J.Y., Shu, Z.R., Chan, P.W., Wu, J.R. and Li, Q.S. (2019) A comparison of micrometeorological methods for marine roughness estimation at a coastal area. *Journal of Wind Engineering and Industrial Aerodynamics*, 195, 104010.

Hofsäß, M., Clifton, A. and Cheng, P.W. (2018) Reducing the uncertainty of lidar measurements in complex terrain using a linear model approach. *Remote Sensing*, 10(9), 1465.

Kodama, Y., Wendler, G. and Ishikawa, N. (1989) The diurnal variation of the boundary layer in summer in Adélie land, eastern Antarctica. *Journal of Applied Meteorology*, 28(1), 16–24.

Lapworth, A. (2005) The diurnal variation of the marine surface wind in an offshore flow. *Quarterly Journal of the Royal Meteorological Society*, 131(610), 2367–2387.

Lapworth, A. (2011) Diurnal variation in the marine wind. *Weather*, 66(2), 48–51.

Launiainen, J. and Laurila, T. (1984) Marine wind characteristics in the northern Baltic Sea. *Finnish Marine Research*, 250, 52–86.

Pichugina, Y.L., Banta, R.M., Brewer, W.A., Sandberg, S.P. and Hardesty, R.M. (2012) Doppler lidar–based wind-profile measurement system for offshore wind-energy and other marine boundary layer applications. *Journal of Applied Meteorology and Climatology*, 51(2), 327–349.

Shu, Z.R., Li, Q.S. and Chan, P.W. (2015a) Statistical analysis of wind characteristics and wind energy potential in Hong Kong. *Energy Conversion and Management*, 101, 644–657.

Shu, Z.R., Li, Q.S. and Chan, P.W. (2015b) Investigation of offshore wind energy potential in Hong Kong based on Weibull distribution function. *Applied Energy*, 156, 362–373.

Shu, Z.R., Li, Q.S., He, Y.C. and Chan, P.W. (2016) Observations of offshore wind characteristics by Doppler-LiDAR for wind energy applications. *Applied Energy*, 169, 150–163.

Shu, Z.R., Li, Q.S., He, Y.C. and Chan, P.W. (2018a) Investigation of low-level jet characteristics based on wind profiler observations. *Journal of Wind Engineering and Industrial Aerodynamics*, 174, 369–381.

Shu, Z.R., Li, Q.S., He, Y.C. and Chan, P.W. (2018b) Observational study of veering wind by Doppler wind profiler and surface weather station. *Journal of Wind Engineering and Industrial Aerodynamics*, 178, 18–25.

Yeo, D.H. and Simiu, E. (2010) *Database-assisted Design for Wind: veering effects on high-rise structures*. Technical Note No. [NIST TN]-1672.

Yu, R., Li, J. and Chen, H. (2009) Diurnal variation of surface wind over central eastern China. *Climate Dynamics*, 33(7–8), 1089–1097.

Yu, T.W. and Wagner, N.Y. (1970) Diurnal variation of onshore wind speed near a coastline. *Journal of Applied Meteorology*, 9 (5), 760–766.